

See discussions, stats, and author profiles for this publication at: <https://www.researchgate.net/publication/231673064>

# Preparation of Chemical Gradient Surfaces by Hyperthermal Polyatomic Ion Deposition: A New Method for Combinatorial Materials Science

ARTICLE *in* LANGMUIR · AUGUST 2001

Impact Factor: 4.46 · DOI: 10.1021/la010592e

---

CITATIONS

51

---

READS

38

3 AUTHORS, INCLUDING:



Erick R. Fuoco

City Colleges of Chicago

12 PUBLICATIONS 288 CITATIONS

SEE PROFILE

# Preparation of Chemical Gradient Surfaces by Hyperthermal Polyatomic Ion Deposition: A New Method for Combinatorial Materials Science

Muthu B. J. Wijesundara, Erick Fuoco, and Luke Hanley\*

Department of Chemistry (mc 111), University of Illinois at Chicago,  
Chicago, Illinois 60607-7061

Received April 23, 2001. In Final Form: July 26, 2001

$\text{C}_3\text{F}_5^+$  ion deposition at 50 eV is used to produce chemical gradient surfaces on poly(methyl methacrylate) (PMMA) by systematic variation of the fluence across the surface. The gradient is characterized by recording small spot X-ray photoelectron spectra and air/water contact angles along the sample length. The fluorine content grows with ion fluence toward the modified end of the sample while the oxygen content decreases simultaneously. These two effects are attributed to the formation of a fluorocarbon film on top of the PMMA surface, which increases in coverage with  $\text{C}_3\text{F}_5^+$  ion fluence. The air/water contact angle increases in parallel with the fluorine content along the surface gradient. These results clearly indicate that a chemical and wettability gradient is produced on PMMA by mass-selected hyperthermal ion deposition.  $\text{C}_3\text{F}_5^+$  ion deposition can also be used to produce chemical gradient surfaces on polystyrene, aluminum, and silicon substrates. It is shown that hyperthermal polyatomic ion deposition is a general method for a wide range of surface chemical gradients on various substrates including polymers, metals, semiconductors, and ceramics.

## I. Introduction

A gradient surface displays a gradual change in its chemical and physical properties along its length. Gradient surfaces have a wide range of applications in combinatorial chemistry and materials science. The preparation of gradient surfaces first began to attract wide attention with the preparation of a wettability gradient.<sup>1</sup> In this paper we demonstrate the deposition of hyperthermal, mass-selected  $\text{C}_3\text{F}_5^+$  ions to produce chemical gradient surfaces on poly(methyl methacrylate) (PMMA) by systematic variation of the fluence across the surface. We also show that polyatomic ion deposition is a general method for the production of chemical gradient surfaces by examining the reactivity of  $\text{C}_3\text{F}_5^+$  ions with polystyrene, aluminum, and silicon substrates.

The surface modification of materials is an essential step for many technological applications including the fabrication of microelectronic devices, biomaterials, composites, and protective coatings. For example, fluorocarbon thin films have been produced that display protective, protein-resistant, low dielectric constant, optical, or gas semipermeable properties.<sup>2</sup> Tailoring the properties of a surface to obtain specific chemistry, roughness, crystallinity, conductivity, or lubricity can be achieved by many different methods, each with its own advantages and disadvantages. Ion beam processing for surface modification has drawn substantial interest due to its experimental flexibility and controllability.<sup>3,4</sup> For example, the decomposition of self-assembled monolayers by atomic ions has been used for lithographic patterning.<sup>5</sup> The soft landing of intact individual polyatomic ions on self-assembled

monolayers has also been demonstrated.<sup>6–8</sup> The chemical modification or growth of thin films on polymer surfaces has also been achieved by hyperthermal polyatomic ions.<sup>9–11</sup> We have previously examined the chemistry, morphology, and stability of fluorocarbon films formed on polystyrene by hyperthermal polyatomic ion deposition.<sup>12–15</sup> We found that the fluorocarbon film chemistry depends on projectile ion energy, structure, and fluence. We observed mostly intact projectile ions deposited onto the surface at low kinetic energy (25 eV) while mostly projectile fragments deposited at higher energy (100 eV). Molecular dynamics simulations supported these results. We also found that ion-deposited fluorocarbon films underwent only minimal oxidation when exposed to the atmosphere, leading to incorporation of only a few percent oxygen into the film over a period of several months.

We describe in this paper a novel method for the production of chemical gradient surfaces by polyatomic ion deposition. The main advantage of a gradient surface is that a single sample can be used to examine the effect of varying a surface parameter across a wide range. This approach drastically reduces both experimental time and

\* To whom correspondence may be addressed. E-mail: L.Hanley@uic.edu.

(1) Elwing, H.; Welin, S.; Askendal, A.; Nilsson, U.; Lundstrom, I. *J. Colloid Interface Sci.* **1987**, *119*, 203–211.

(2) Chan, C.-M.; Ko, T.-M.; Hiraoka, H. *Surf. Sci. Rep.* **1996**, *24*, 1–54.

(3) Rabalais, J. W. *Low Energy Ion-Surface Interactions*; Wiley: Chichester, 1994.

(4) Hanley, L.; Sinnott, S. B. *Surf. Sci.*, in press.

(5) Ada, E. T.; Hanley, L.; Etchin, S.; Melngailis, J.; Dressick, W. J.; Chen, M.-S.; Calvert, J. M. *J. Vac. Sci. Technol., B* **1995**, *13*, 2189–2196.

(6) Miller, S. A.; Luo, H.; Pachuta, S. J.; Cooks, R. G. *Science* **1997**, *275*, 1447–1450.

(7) Luo, H.; Miller, S. A.; Cooks, R. G.; Pachuta, S. J. *Int. J. Mass Spectrom. Ion Processes* **1998**, *174*, 193–217.

(8) Shen, J.; Yim, Y. H.; Feng, B.; Grill, V.; Evans, C.; Cooks, R. G. *Inter. J. Mass Spectrom. Ion Processes* **1999**, *182/183*, 423–435.

(9) Nowak, P.; McIntyre, N. S.; Hunter, D. H.; Bello, I.; Lau, W. M. *Surf. Interface Anal.* **1995**, *23*, 873–878.

(10) Lau, W. M.; Kwok, R. W. M. *Inter. J. Mass Spectrom. Ion Processes* **1998**, *174*, 245–252.

(11) Ada, E. T.; Kornienko, O.; Hanley, L. *J. Phys. Chem. B* **1998**, *102*, 3959–3966.

(12) Wijesundara, M. B. J.; Hanley, L.; Ni, B.; Sinnott, S. B. *Proc. Natl. Acad. Sci. U.S.A.* **2000**, *97*, 23–27.

(13) Wijesundara, M. B. J.; Ji, Y.; Ni, B.; Sinnott, S. B.; Hanley, L. *J. Appl. Phys.* **2000**, *88*, 5004–5016.

(14) Hanley, L.; Fuoco, E.; Wijesundara, M. B. J.; Beck, A. J.; Brookes, P. N.; Short, R. D. *J. Vac. Sci. Technol., A* **2001**, *19*, 1531–1536.

(15) Wijesundara, M. B. J.; Zajac, G.; Fuoco, E.; Hanley, L. *J. Adhes. Sci. Technol.* **2001**, *15*, 599–612.

methodological errors.<sup>16</sup> The use of continuous or stepped gradient surfaces is a central technique in combinatorial chemistry and materials science.<sup>17,18</sup> The combinatorial approach leads to rapid technological development with improved efficiency and lower research cost. For example, the development of new biomaterials requires the evaluation of the biocompatibility of a large number of samples. Gradient surfaces have been used to minimize the number of samples required for these biocompatibility studies.<sup>16</sup>

Several methods have been described for the preparation of gradient surfaces, including palladium deposition, diffusion, density gradients, plasmas, and corona discharges.<sup>16,19,20</sup> Recently, a spatial gradient in electrochemical potential has been used to create a surface chemical potential gradient via electrochemical desorption of alkanethiols.<sup>21</sup> We discuss here a novel method for preparation of gradient surfaces on a wide range of substrates by mass-selected, hyperthermal polyatomic ion deposition. We use mass-selected 50 eV  $C_3F_5^+$  ions to produce a chemical gradient surface on PMMA by systematic variation of the ion fluence along the sample length. Fluorination of PMMA surfaces has been considered, for example, in the production of artificial intraocular lenses.<sup>2,22,23</sup> Native PMMA presents a relatively hydrophilic surface whereas fluorocarbon ion-modified PMMA becomes hydrophobic. We explore the potential of extending our gradient surface preparation technique to other substrates by studying the modification of polystyrene, silicon, and aluminum. We also discuss the general application of polyatomic ion deposition to the production of a wide array of surface chemical gradients. We employ small spot X-ray photoelectron spectroscopy to determine the systematic change in surface chemistry along the gradient surface. We use air/water contact angles to determine the change in wettability along the gradient surface.

## II. Experimental Section

**A. Thin Film Preparation and Ion Deposition.** Thin polymer films are spin coated onto Si(100) wafers from 2.0% poly(methyl methacrylate) (PMMA, 350 kDa, Aldrich) solution in *o*-xylene and 0.3% polystyrene (PS, 4.6 kDa, Aldrich) solution in  $CH_2Cl_2$ , respectively. Spin speeds are 2000 rpm for PMMA and 6000 rpm for PS. The aluminum surface used is common aluminum foil ( $Al/Al_2O_3$ ), which is rinsed in solvents and then cleaned in a vacuum by 500 eV  $Ar^+$  ion sputtering for 30 min at an ion current of 2.0  $\mu A$ . The silicon surfaces are prepared by etching Si(100) wafers in 5% HF solution followed by rinsing with deionized water, to remove the native oxide and produce a hydrogen-terminated surface, H-Si(100).<sup>24</sup> Survey X-ray photoelectron scans are performed to confirm the cleanliness of these substrates prior to ion exposure (see below).

The experimental apparatus used to perform ion deposition and surface analysis is described elsewhere.<sup>13</sup> Briefly, it consists of a differentially pumped, hyperthermal ion source attached to

two distinct vacuum chambers for sample preparation and surface analysis. The  $C_3F_6$  precursor gas (Matheson) is ionized by 80 eV electron impact ionization, the ions are accelerated to 1 keV, then the  $C_3F_5^+$  ions are velocity-selected by a Wien filter. The  $C_3F_5^+$  ions are then decelerated to 50 eV ion energy, refocused, and transmitted at normal incidence to the target mounted in the preparation chamber. A low energy electron flood gun is used to compensate for ion-induced charging. The preparation chamber pressure typically increases from  $\sim 0.5$  to  $\sim 8 \times 10^{-8}$  Torr during ion bombardment due to background  $C_3F_6$  gas from the ion source. Control experiments confirm that no significant film deposition or surface modification is caused by  $C_3F_6$  background gas or the neutralizing electron beam. Typical ion currents are 15–20 nA during ion exposure. The chemical gradient on the PMMA surface is created by linearly increasing the  $C_3F_5^+$  ion fluence from 0 to  $2.0 \times 10^{15}$  ions/cm<sup>2</sup> across the sample surface. Ion fluence for all other surfaces is  $2.0 \times 10^{15}$  ions/cm<sup>2</sup> except for the fluence-dependent studies on PS, which vary from 1.0 to  $4.0 \times 10^{15}$  ions/cm<sup>2</sup>. All ion-modified substrates are transferred directly to the analysis chamber for XPS analysis, without any air exposure.

**B. X-ray Photoelectron Spectroscopy (XPS).** XPS data acquisition and analysis have been previously discussed in detail<sup>12,13</sup> and therefore only briefly summarized here. All XPS data are obtained using a high-resolution monochromatic Al K $\alpha$  X-ray source (15 keV, 25 mA emission current, model VSW MX10 with 700 mm Rowland circle monochromator, VSW Ltd., Macclesfield, Cheshire, U.K.) with a 150 mm concentric hemispherical analyzer (model Class 150, VSW Ltd.) equipped with multichannel detector operated at constant energy analyzer mode. The photoemission angle is normal to the surface and the pass energy is kept at 22 eV, which gives a 0.75 eV energy resolution for the Ag (3d<sub>5/2</sub>) photoemission peak on a clean polycrystalline Ag foil. Control experiments confirm that there is no X-ray damage to any of the films during a typical XPS acquisition time of 2–3 h.<sup>13</sup> All binding energies given here are referenced to the C(1s) core level photoemission peak of the aliphatic/aromatic/graphitic carbon peak at 285.0 eV. Peak fitting is done using the Spectra software with Shirley background and 35:65 Lorentzian:Gaussian product line shape. Elemental concentration is estimated using elemental sensitivity factors,<sup>25</sup> and the transmission function for the electron energy analyzer (VSW). Two samples are run for each reported data point and the errors shown correspond to their standard deviation.

**C. Contact Angle Measurements.** All air/water contact angle measurements are made at room temperature using the sessile drop (10  $\mu L$ ) and half-angle measuring method with a projection screen and 12:1 magnification (model CAM-MICRO, Tantec, Schaumburg, IL). The accuracy of the contact angle measurements is  $\pm 2^\circ$ , and the measuring range of this instrument is  $10^\circ$  to  $120^\circ$ . The recorded contact angle is the average of four measurements.

## III. Results and Discussion

**A. Gradient Surface of PMMA.** A poly(methyl methacrylate) (PMMA)–fluorocarbon (FC) chemical gradient surface is produced on PMMA by  $C_3F_5^+$  ion exposure as a function of distance from the unmodified end to the highly modified end. The gradient is created by linearly increasing the  $C_3F_5^+$  ion fluence across the sample surface. The gradient is characterized by recording small spot X-ray photoelectron spectra (XPS) and air/water contact angles along the sample length.

Figure 1 shows the survey XPS of the PMMA–FC gradient surface at various spots from the unmodified (PMMA) to modified (FC) end. The inset of Figure 1 displays the high-resolution C(1s) core level XPS of the same sample positions. The survey scans in Figure 1 display carbon and oxygen for all sample points. Fluorine is absent from the unmodified PMMA end of the sample. The fluorine content grows with ion fluence toward the modified end of the sample while the oxygen content

(16) Ruardy, T. G.; Schakenraad, J. M.; Mei, H. C. v. d.; Busscher, H. J. *Surf. Sci. Rep.* **1997**, *29*, 1–30.

(17) van Dover, R. B.; Schneemeyer, L. F.; Fleming, R. M. *Nature* **1998**, *392*, 162–164.

(18) Jandeleit, B.; Schaefer, D. J.; Powers, T. S.; Turner, H. W.; Weinberg, W. H. *Angew. Chem., Int. Ed.* **1999**, *38*, 2494–2532.

(19) Chaudhury, M. K.; Whitesides, G. M. *Science* **1992**, *256*, 1539–1542.

(20) Liedberg, B.; Wirde, M.; Tao, Y.-T.; Tengvall, P.; Gelius, U. *Langmuir* **1995**, *13*, 5329–5334.

(21) Terrill, R. H.; Balss, K. M.; Zhang, Y.; Bohn, P. W. *J. Am. Chem. Soc.* **2000**, *122*, 988–989.

(22) Brinen, J. S.; Greenhouse, S.; Pinatti, L. *Surf. Interface Anal.* **1991**, *17*, 63–70.

(23) Li, D. J.; Cui, F. Z.; Gu, H. Q. *Biomaterials* **1999**, *20*, 1889–1896.

(24) Bello, I.; Chang, W. H.; Lau, W. M. *J. Vac. Sci. Technol., A* **1994**, *12*, 1425–1430.

(25) Scofield, J. H. *J. Electron Spectrosc. Relat. Phenom.* **1976**, *8*, 129–137.

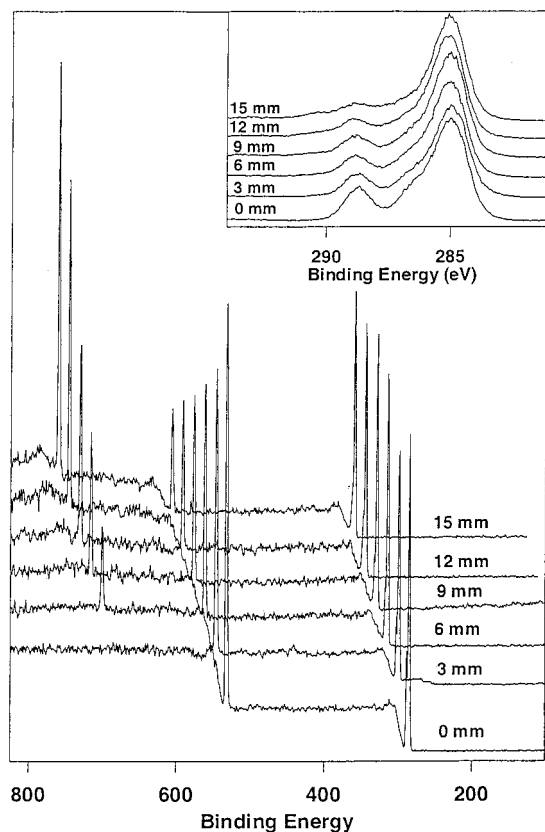


**Figure 1.** Survey X-ray photoelectron spectra of 50 eV  $C_3F_5^+$  ion modified poly(methyl methacrylate) (PMMA) at six different spots from the unmodified (PMMA) to modified (FC) end along the sample length. Inset is the C(1s) core level XPS at the same sample positions.

decreases simultaneously. However, the amount of total carbon on the surface varies only slightly along the surface. The inset of Figure 1 displays the C(1s) core level XPS at various points across the surface chemical gradient. These C(1s) core levels also display a chemical change with ion fluence, which will be discussed further in the next section.

The elemental composition of the gradient surface is calculated at 11 spots separated by 1.5 mm intervals along the sample length by using C(1s), O(1s), and F(1s) XPS peak areas from data similar to that shown in Figure 1. The XPS spot size is slightly less than 2 mm, minimizing the overlap of adjacent spots. Figure 2 displays the carbon, fluorine, and oxygen percentages along with the air/water contact angle recorded at each spot, plotted as a function of distance along the gradient surface from the unmodified end. Figure 2 indicates that the total fluorine on the surface increases with ion fluence. By contrast, the total oxygen content decreases with increasing ion fluence. These two effects are attributed to the formation of a FC film on top of the PMMA surface. The coverage and thickness of this FC film increase with  $C_3F_5^+$  ion fluence. Figure 2 also indicates that total carbon on the surface stays relatively constant along the gradient surface, since fluorine incorporation is associated with carbon incorporation due to the composition of the incident ion.

The XPS data clearly shows a gradual increase in FC content occurring simultaneous with a decrease in oxygen along the gradient surface. Air/water contact angles are also used to demonstrate the existence of the gradient. Figure 2 shows the air/water contact angle increases in parallel with the fluorine content on the PMMA surface. Native PMMA has been previously shown to display a 72° air/water contact angle whereas FC films grown on PMMA

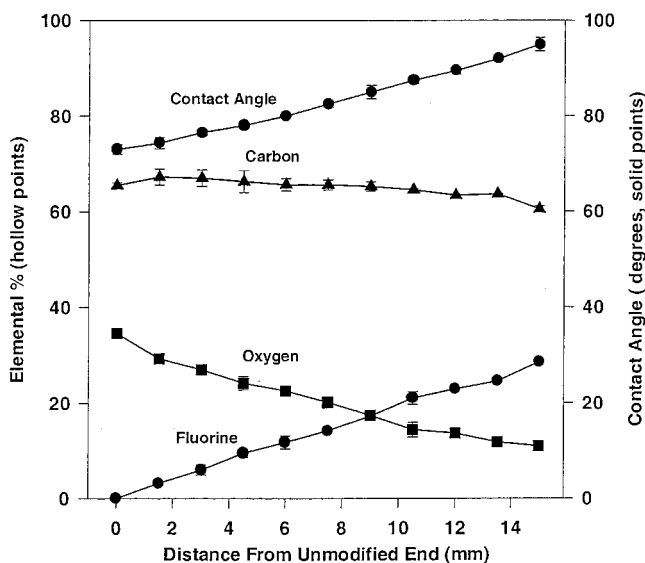


**Figure 2.** Percentages of total carbon, fluorine, and oxygen on the gradient PMMA surface produced by 50  $C_3F_5^+$  at various sample positions. Uppermost data are the air/water contact angle at the same sample positions.

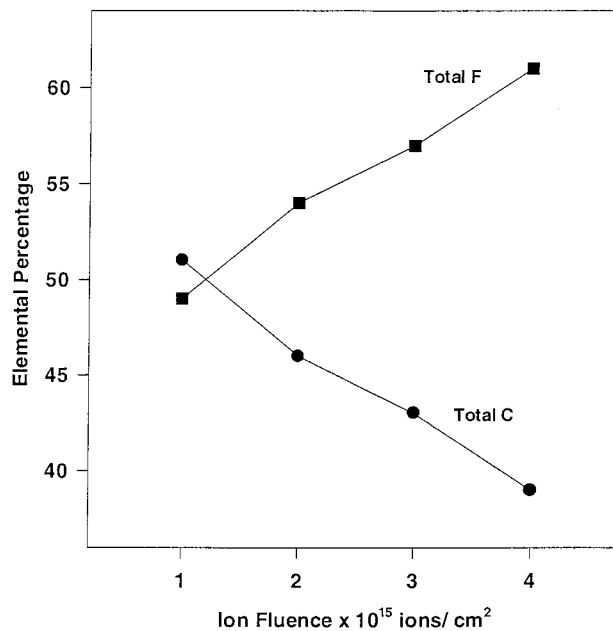


**Figure 3.** Percentages of total carbon and fluorine on 50 eV  $C_3F_5^+$  ion modified polystyrene (PS) surfaces, at fluence ranging from  $(1.0 \text{ to } 4.0) \times 10^{15} \text{ ions/cm}^2$ .

from plasmas displayed a maximum 109° air/water contact angle.<sup>22</sup> Similarly, the gradual decrease in hydrophilicity that accompanies the introduction of FC onto the PMMA surface leads to the contact angle gradient displayed in Figure 2. The maximum air/water contact angle measured on our gradient surface is 95°, below the 109° value previously observed on a FC-covered PMMA.<sup>22</sup> The relatively low value of this maximum contact angle and the fact that it did not plateau with increasing ion fluence indicate that either the PMMA surface is still not completely covered with the FC film or the FC film properties are still changing with ion fluence.

Figure 3 displays the fluorine and carbon content from XPS data recorded for a 50 eV  $C_3F_5^+$  ion-modified polystyrene (PS) surface as a function of ion fluence ranging from  $1.0 \text{ to } 4.0 \times 10^{15} \text{ ions/cm}^2$ .<sup>13</sup> Figure 3 clearly indicates that total fluorine content increases while carbon



**Table 1. Percentage Elemental Composition of PS, PMMA, Al, and Si Native Surfaces and after C<sub>3</sub>F<sub>5</sub><sup>+</sup> Ion Exposure, by XPS Peak Area Analysis**

substrate	native			after C <sub>3</sub> F <sub>5</sub> <sup>+</sup> ion modification			
	C	O	Al or Si	C	O	F	Al or Si
PS	100			46 ± 1.1		54 ± 0.9	
PMMA	66 ± 0.6	35 ± 0.6		56 ± 1.1	11 ± 0.4	34 ± 1.5	
Si	5 ± 1.2	4 ± 0.7	91 ± 0.5	27 ± 1.6		57 ± 1.0	15 ± 1.4
Al		60 ± 0.7	38 ± 0.4	5 ± 0.3	42 ± 0.2	21 ± 1.1	31 ± 0.5

content on the surface decreases as the ion fluence increases, implicating fluence as the source of the chemical gradients observed above. This result also indicates that C<sub>3</sub>F<sub>5</sub><sup>+</sup> ion deposition can also be used to produce gradient surfaces on PS, which we have also observed (data not shown).

We have not directly measured the thickness or nano-scale morphology of the FC films formed on PMMA. FC films formed on PS by 50 eV C<sub>3</sub>F<sub>5</sub><sup>+</sup> are on the order of ~1 nm thick, with the thickness apparently increasing with ion fluence.<sup>13</sup> Furthermore, atomic force microscopy has shown that FC films on PS are spatially homogeneous down to ~10 nm, with the heterogeneity defined by the macroscopic profile of the ion beam.<sup>15</sup> Given the chemical similarity of the FC films formed on PS and PMMA (see below), the film morphology is also likely to be similar.

**B. Comparing C<sub>3</sub>F<sub>5</sub><sup>+</sup> Ion Modification of Several Substrates.** We show above that mass-selected hyperthermal ion deposition can produce chemical gradients on PMMA and PS polymer surfaces by varying the ion fluence. To explore the possibility of extending this method, we consider the likelihood of forming similar gradients on other surfaces. We compare the surface chemistry on four different surfaces modified using 50 eV C<sub>3</sub>F<sub>5</sub><sup>+</sup> ions, at a fixed fluence of  $2 \times 10^{15}$  ions/cm<sup>2</sup>. Elemental percentages of native and C<sub>3</sub>F<sub>5</sub><sup>+</sup> ion-modified PS, PMMA, aluminum, and silicon are calculated from the survey XPS and presented in Table 1. The surfaces of all four substrates show a substantial amount of fluorine in all cases. The high-resolution C(1s) spectra are also examined to obtain a more detailed view of how the FC ion modified surface chemistry varies with substrate. We begin by comparing the two polymer surfaces, then we compare the metal with the semiconductor surface.

**Comparing PMMA with PS.** Survey scans and high-resolution XPS for each element present are recorded before and after C<sub>3</sub>F<sub>5</sub><sup>+</sup> ion exposure of PS and PMMA. The elemental compositions of both ion-modified polymer surfaces are given in Table 1. PS displays higher fluorination efficiency (54%) than does PMMA (34%) at the same ion fluence. The chemical nature of these two polymers clearly affects their fluorination efficiency, implying that the aromatic ring in PS may be more amenable to fluorination than is the ester group of PMMA.

Figure 4 displays the C(1s) core level spectra of (a) PMMA and (b) PS before and after ion deposition. The inset of Figure 1 displays the C(1s) core level spectra as they vary along the surface chemical gradient on PMMA. Visual comparison of the C(1s) of both PMMA and PS before and after ion deposition clearly shows the presence of FC functionalities on the ion-modified surface. C(1s) XPS of native PS shows the aliphatic/aromatic hydrocarbon peak at 285.0 eV binding energy and a  $\pi-\pi^*$  transition at 291.8 eV. The C(1s) of C<sub>3</sub>F<sub>5</sub><sup>+</sup> ion modified PS additionally shows a series of well-resolved, higher binding energy shoulders on the C(1s) peak, attributed to various FC functionalities. The actual FC moieties on PS and their binding energies have been previously discussed in detail<sup>13</sup> and are summarized in Table 2. For ion-modified PS films, the 286.2 eV component is attributed to  $\text{CCF}_n$ , 288.7 eV

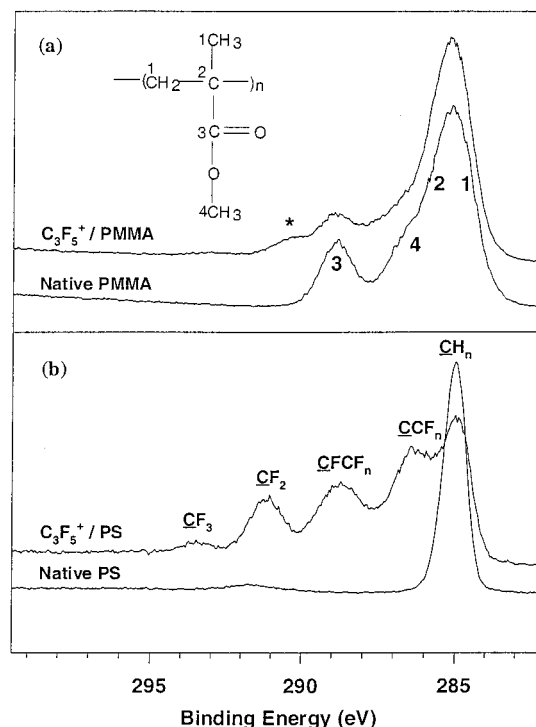


**Figure 4.** The C(1s) core level XPS of PMMA (a) and PS (b) before and after deposition of 50 eV C<sub>3</sub>F<sub>5</sub><sup>+</sup> ions at fluence of  $2.0 \times 10^{15}$  ions/cm<sup>2</sup>. The inset diagram of the PMMA monomer is labeled with the carbon atom numbering scheme.

to  $\text{CFCF}_n$ , 291.1 eV to  $\text{CF}_2$ , and 293.3 eV to  $\text{CF}_3$ . These same C(1s) peak assignments are used for the FC films on all four substrates, except as noted below for PMMA.

The C(1s) of native PMMA (see Figure 4a) shows only three clearly visible peaks, but four peaks are traditionally used for fitting: peak 1 ( $-\text{CH}_2-\text{C}-\text{CH}_3$ ) at 285.0 eV, peak 2 ( $-\text{C}-\text{C}=\text{O}$ ) at 285.9 eV, peak 3 ( $\text{O}-\text{C}=\text{O}$ ) at 289.0 eV, and peak 4 ( $-\text{O}-\text{CH}_3$ ) at 286.8 eV (the detected carbon atom is underlined). The schematic of the PMMA structure shown in the inset of Figure 4 gives the carbon atom numbering scheme. The relative percentages of peaks 1, 2, 3, and 4 are 43%, 21%, 19%, and 17%, respectively. These peak assignments and percentages are generally consistent with literature values.<sup>26,27</sup> Unfortunately, the C(1s) components on ion-modified PMMA attributed to  $\text{CCF}_n$  and  $\text{CFCF}_n$  (appearing at 286.2 and 288.7 eV, respectively) overlap with the  $-\text{C}-\text{C}=\text{O}$  and  $-\text{O}-\text{C}=\text{O}$  components of native PMMA (appearing at 285.9 and 289.0 eV, respectively), due to their natural line widths and the 0.75 eV instrumental energy resolution. The slight offset between the native PMMA and FC peaks leads to apparent broadening in peaks 2–4 as the  $\text{CCF}_n$  and  $\text{CFCF}_n$  moieties appear on the surface. Additionally, at least one new peak appears at 290.6 eV with C<sub>3</sub>F<sub>5</sub><sup>+</sup> ion exposure.

(26) Rosencrance, S. W.; Way, W. K.; Winograd, N.; Shirley, D. A. *Surf. Sci. Spectrosc.* **1993**, 2, 71–75.

(27) Groning, P.; Kuttel, O. M.; Collaud-Coen, M.; Dietler, G.; Schlappbach, L. *Appl. Surf. Sci.* **1995**, 89, 83–91.

**Table 2. Fluorocarbon Component Percentages of PS, Al, and Si Surfaces after  $C_3F_5^+$  Ion Exposure, by Fitting of C(1s) XPS<sup>a</sup>**

substrate	CH <sub>n</sub> 285.0 eV	CCF <sub>n</sub> 286.2 eV	CFCF <sub>n</sub> 288.7 eV	CF <sub>2</sub> 291.1 eV	CF <sub>3</sub> 293.3 eV
PS	33 ± 1	34 ± 1	19 ± 1	12 ± 1	1.0 ± 0.1
Si	0	42 ± 4	36 ± 3	18 ± 1	3.6 ± 0.2
Al	25 ± 3	47 ± 1	16 ± 1	8.3 ± 0.3	3.1 ± 0.1

<sup>a</sup> All films showed only one carbon component prior to ion bombardment.

**Table 3. Chemical Composition of PMMA Surface, Both Native and after  $C_3F_5^+$  Ion Exposure, by Deconvolution of C(1s) XPS**

substrate	#1: CH <sub>n</sub> 285.0 eV	#2: C-C=O, #4: O-CH <sub>3</sub> , & CCF <sub>n</sub> 286.2 eV	#3: O-C=O & CFCF <sub>n</sub> 288.7 eV	OCFCF <sub>n</sub> 290.6 eV	CF <sub>2</sub> 291.1 eV	CF <sub>3</sub> 293.3 eV
native	44 ± 1	39 ± 1	17 ± 1	0	0	0
ion modified	46 ± 1	37 ± 1	14 ± 1	3 ± 0.1	0	0

Fluorination of oxygenated carbon occurs on PMMA, leading to the formation of  $C_xF_yO_z$  groups. The 290.6 eV peak appears between the  $CF_2$  and  $CFCF_n$  components and may be attributed to formation of  $OCFCF_n$ . Other  $C_xF_yO_z$  groups are also expected here which will contribute to the aforementioned peak broadening even though they cannot be resolved. Table 3 quantifies the chemical modification of PMMA via fitting of the C(1s) spectra for native and ion-modified PMMA. The two sets of overlapped native PMMA and FC peaks are fit using single peaks at the same binding energies employed above for  $CCF_n$  and  $CFCF_n$ .  $CF_2$  and  $CF_3$  are fit with peaks at 291.1 and 293.3 eV, respectively, and the new  $OCFCF_n$  peak is fit using a peak at 290.6 eV.

Table 3 shows that the new  $OCFCF_n$  peak accounts for 3% of the total surface carbon, growing at the expense of all the other PMMA peaks. No  $CF_2$  or  $CF_3$  is detected on the ion-modified PMMA surface. This result indicates that the ester group is preferentially modified by ion bombardment. It was previously argued that preferential decomposition of the ester group by  $\sim 10$  eV  $Ar^+$  ions leads to a decrease in oxygen content on PMMA.<sup>27</sup> This preferential decomposition was attributed to an ion-induced dipole in the ester group that increased its collision cross section with respect to the aliphatic groups on PMMA. A similar effect may occur here for  $C_3F_5^+$  modification of PMMA but depends on the  $C_3F_5^+$  ions maintaining their charge upon impact. However, if the  $C_3F_5^+$  ion neutralizes before impact, as may occur here, then such ion-dipole effects will be limited. An alternative explanation is that the ester group is simply more reactive with the neutralized, energetic  $C_3F_5$ , even in the absence of ion-induced dipole effects. A decrease in oxygen attributed to decomposition of C=O groups was observed when PMMA was bombarded by 40 keV  $F^+$  ions.<sup>28</sup> However, the use of an atomic projectile and much higher kinetic energy is expected to dramatically alter the ion-surface interaction when compared with the hyperthermal polyatomic ions employed here.<sup>4</sup>

**Comparing Aluminum with Silicon.** Comparison of the ion deposition on aluminum, Al/Al<sub>2</sub>O<sub>3</sub>, with silicon, H-Si(100), is done to demonstrate the general feasibility of producing gradient surfaces on metal and semiconductor surfaces. Survey spectra of the aluminum foil show only aluminum and oxygen before ion deposition (Table 1). Surface XPS of the silicon wafer shows mainly silicon with only slight amounts of residual carbon and oxygen on the surface (data not shown). Survey scans of both substrates after  $C_3F_5^+$  ion deposition indicate a significant amount

of fluorine, with the calculated elemental percentages summarized in Table 1. The aluminum and silicon surfaces display 21% and 57% fluorine after exposure at the same ion fluence, respectively. Thus, the fluorination efficiency is nearly three times higher for silicon than for aluminum. The C/F elemental ratio of ion-deposited FC film is 1:4 and 1:2 on aluminum and silicon, respectively. Thus, the FC film composition on silicon somewhat resembles that of the projectile ion. However, the FC film composition on aluminum displays much more fluorine than carbon and does not resemble the incident ion at all. The fluorination efficiency and fragmentation behavior are affected by the collision dynamics, which are affected by the surface hardness and reactivity and lead to differences in ion scattering, deposition, penetration, and surface bonding.

Covalent attachment of FC to these substrates can be further examined by studying the changes in the Al(2p) and Si(2p) core level XPS (not shown). The Al(2p) peak of the aluminum foil displays two components, a sharp component for metallic Al due to the bulk at 72.0 eV (0.7 eV fwhm) and a broader component due to the Al<sub>2</sub>O<sub>3</sub> surface layer at 74.8 eV (1.4 eV fwhm). With  $C_3F_5^+$  ion exposure, the Al<sub>2</sub>O<sub>3</sub> component shifts to a 0.6 eV high binding energy and its width increases by 0.2 eV. These changes are attributed to covalent attachment of either fluorine or FC to the aluminum. There are no significant changes to the Si(2p) photoemission peak due to ion exposure, as has been seen previously in hyperthermal  $CF_3^+$  bombardment of silicon surfaces.<sup>24</sup>

The C(1s) core level XPS are also recorded on aluminum and silicon following  $C_3F_5^+$  ion exposure. Both C(1s) spectra display high binding energy features for FC functionalities, with the same binding energies as those seen for PS. Table 2 represents the percentages of each FC component of FC film on aluminum and Si, indicating that the composition of the FC film differs significantly between aluminum and silicon. The FC film on silicon is composed only of the four FC components, without any nonfluorinated carbon. By contrast, the FC film on aluminum displays both the four FC components and aliphatic carbon. The lower amount of highly fluorinated  $CF_2$  and  $CF_3$ , and the higher amount of less fluorinated  $CFCF_n$  and  $CCF_n$  on aluminum further confirm the higher fragmentation of the projectile ion (see above). FC films of similar chemical composition have been observed from plasma deposition onto aluminum<sup>29</sup> and silicon<sup>24,30</sup> substrates.

(29) O'Keefe, M. J.; Rigsbee, J. M. *J. Appl. Polym. Sci.* **1994**, *53*, 1631–1638.

(30) Schaepkens, M.; Standaert, T. E. F. M.; Rueger, N. R.; Sebel, P. G. M.; Oehrlein, G. S.; Cook, J. M. *J. Vac. Sci. Technol., A* **1999**, *17*, 26–37.

(28) Li, D. J.; Cui, F. Z.; Gu, H. Q. *Nucl. Instrum. Methods Phys. Res., Sect. B* **1999**, *152*, 80–88.

Our results confirm that we produced FC films on both aluminum and silicon surfaces from FC ions, although the efficiency and the film chemistry vary. These results show that polyatomic ions can be used for producing gradients on metal and semiconductor surfaces, although the chemistry of the gradient will depend on the ion, substrate, and kinetic energy.

#### IV. Conclusions

This study shows it is possible to produce chemical gradient surfaces by deposition of mass-selected hyperthermal polyatomic ions. We successfully obtain a wettability gradient on poly(methyl methacrylate) using mass-selected  $\text{C}_3\text{F}_5^+$  ion deposition by varying the ion fluence. We also show that polyatomic ion deposition is a promising method for producing gradient surfaces on other polymeric and nonpolymeric materials. We previously found that the chemical nature of the ion-deposited film can be controlled by varying the ion energy and structure.<sup>12,13</sup> We observed that surface chemistry and fluorination efficiency on polystyrene changes with incident ion energy,

with the intact ion modifying the substrate at low kinetic energies. This method is not limited to one particular type of polyatomic ion because in addition to  $\text{C}_3\text{F}_5^+$ , we have already studied the modification of various surfaces by  $\text{SF}_5^+$ ,  $\text{SO}_3^+$ ,  $\text{CF}_3^+$ , and  $\text{Si}_2\text{O}(\text{CH}_3)_5^+$  ions.<sup>11–14</sup> The fact that intact individual polyatomic ions can be soft-landed on certain substrates further implies the diverse range of chemical gradients available to polyatomic ion deposition.<sup>6–8</sup> Insulating substrates can utilize our method in conjunction with a low-energy electron beam for charge neutralization. Overall, polyatomic ion deposition may be used in cases where existing methods<sup>16,19–21</sup> either do not allow sufficient control over the gradient distribution or do not work for a desired surface chemistry or substrate.

**Acknowledgment.** This work was supported by the National Science Foundation through Grant CHE-9986226. We thank Tejal Desai for use of her contact angle apparatus.

LA010592E